

NANO-SCALE PARTICULATE MATTERS FOUND IN URBAN STREET DUST IN CLUJ – NAPOCA, ROMANIA

**Alexandra Gertrud HOSU PRACK^{1*}, Ioan PETEAN¹, George ARGHIR²,
Liviu Dorel BOBOS¹, & Maria TOMOAI COTISEL¹**

¹*Babeş-Bolyai University of Cluj-Napoca, Faculty of Chemistry and Chemical Engineering, Arany Janos Str, No.11, Cluj-Napoca, Romania. * Corresponding author: pgertrud@gmail.com*

²*Technical University of Cluj – Napoca, Faculty of Materials and Environment Engineering, Muncii Ave. No.103 – 105, Cluj – Napoca, Romania.*

Abstract: The urban environment contains several sources of particulate matters (PM). The street dust (SD) summarizes particles from all PM sources in urban area. Our present research is focused on the street dust collected from Piata Garii in Cluj Napoca in autumn. The particle distribution analysis shows that 60.84 % of the collected SD is gross (over 200 µm diameter), only a small fraction of 0.83 % is situated below 64 µm diameter. Even a small rate of this could be harmful considering the street dust amount reported for all square surfaces. The mineral components were identified by X-ray diffraction: quartz, muscovite, calcite, kaolinite and lepidocrocite. Finest particles were trapped on the solid substrate (e.g. glass) by adsorption from a SD dispersion in deionized water. The obtained PM film was investigated both by AFM microscopy and X-ray diffraction. Our findings suggest that a thin layer of nano – scaled PM containing finest quartz particles and finest clay fragments is adsorbed on the glass. The average diameter of nano – scaled PM is situated at 95 nm for quartz and around 45 nm for clay particles. As a final remark all these ultra fine PM are sensitive to humidity proving the cohesive tendency to form bigger particles. This could be a way to reduce their propagation in air.

Keywords: street dust PM, nanoparticles, atomic force microscopy (AFM)

1. INTRODUCTION

The scientific interest is focused on the finest particles with environmental impact, which are able to harm living beings. The finest material particles able to be found by physical methods are nanoparticles. They are used at large scale in nanotechnology applications in various directions such as biomaterials, environmental energy sources and many more (Linkov et al., 2013). The toxicity of ultra fine particles is caused by their ability to penetrate the living tissues membranes (Buzea et al., 2007; Pauluhn 2009, Yah et al., 2012). Such kind of toxicity is useful in the targeted treatment of the carcinogenic tumors (Smith et al., 2013) but their presence in the free environment could be dangerous for the human health. The question would be how to reach nanoparticles in the open environment. The concept of ultra fine particles formed up by the fragmentation of usually micro particles under the

environmental factors could lead to such particles. Therefore, the outline could be followed among the atmospheric PM 10 and PM 2.5.

European Union has elaborated a comprehensive direction for the monitoring and studying of air particulate matters. Most of developed studies are focused on PM10 and PM 2.5, revealing the mineral and chemical composition as well as particle distribution (Vardoulakis & Kassomenos 2008; Gidhagen et al., 2009; Joshi et al., 2009; Carvalho et al., 2011). Particulate matters prove to be more effective in the air pollution as could be observed in the air policies from early fifties to the present (Williams 2004). Such air solid dispersions could be dangerous for human health increasing the risk of lungs and cardiovascular diseases (Hartog et al., 2003; Polichetti et al., 2009). Many of these health risks are significant increased by the presence of ultra fine particles. Polichetti et al., 2009 mention the presence of PM 1, meaning

particles with diameter of 1µm and below. Several studies were conducted to trace such finest particles (e.g. PM1) in air dispersions (Vecchi et al., 2004; Giugliano et al., 2005). Recent studies reveal that transport traffic is one of the major causes which of air particulate dispersion forming (Hosu-Prack et al., 2010; Muntean et al., 2012; Jancsek-Turoczi et al., 2013). It was pointed out the relation between the street dust and the air PM formation. We aim to reveal and characterize the nanoparticles in the street dust collected from a high circulated square in Cluj–Napoca city (Romania).

2. METHODS

The street dust samples (SD) were collected weekly from the Railway Station Square Cluj–Napoca from 28 October 2010 to 25 November 2010. The samples were collected with polymeric broom and pan from a large area of Piata Garii. We refer to SD1 to the sample collected in the first week, and SD2 to the sample collected in the third week of the interval. Finally an average sample were (ASD) prepared by mixing equal quantities of SD from the samples collected in each week of the sampling interval. These samples are relevant for autumnal behavior of PM in the urban environmental conditions. It is the starting point for an enlarged new study, which will be developed beginning with October 2015 for six months.

The microscopic particles distribution was performed on the successive sieves having mesh ratio progress 0.25 according to the standard prescriptions SR EN 933-1:2002/A1:2006. The successive mesh dimensions are: 200; 160; 125; 100; 80, and 64 µm.

The nanoparticles transfer in a thin film is a difficult matter due to various physic – chemical parameters. There are some methods such drop spreading, horizontal and vertical adsorption and Langmuir Blodgett Techniques (Tomoaia et al., 2011; Mocanu et al., 2012). Our previous study used the sedimentation of the bigger particles meanwhile finest one remains in dispersion, followed by drop spreading on the solid substrate (Hosu Prack et al., 2010). We observe that finest particles adsorption from aqueous dispersion to solid substrate (e.g. glass) presents the best features for AFM investigation, and could be suitable for X-ray diffraction as well. Thus, the finest particles samples were prepared by vertical adsorption from ASD aqueous dispersion for 10 seconds, followed by natural drying. A particle thin layer (PTL) results in this manner. The dispersion was prepared by intensive stirring of 10 g of ASD in 100 ml of deionized water.

The X-ray diffraction (XRD) analyses were done with a DRON 3 diffractometer equipped with data acquisition module and Matmec VI.0 software. XRD patterns were obtained with a monochrome Cu_{Kα} radiation in the continuous scan mode, diffraction angle ranges from 20 to 100 degree, scan speed 2 deg/min and time constant 5 seconds. MATCH 1.0 X – ray diffraction database powered by Crystal Impact Company was used for the mineral identification.

The micro structural aspects were observed by optical microscopy and by dark field optical microscopy on an IOR 8 microscope, and the cross polarized light microphotographs were done on a mineralogical Karl Zeiss Jena mineralogical microscope Laboval 2. The images were digitally acquired using a Samsung camera 8 MPx.

Atomic force microscopy (AFM) investigation was done with a JEOL JSPM 4210 Scanning Probe Microscope in tapping mode, using NSC 11 cantilevers with silicon nitride conical tip (Micromasch Co.). The images were recorded and processed in the standard manner according to the JEOL Win SPM 2.0 soft.

3. RESULTS AND DISCUSSIONS

The minerals identification was done by XRD, the resulted diffractograms are presented in figure 1. The diffraction peaks are well formed, proving the crystalline state of the samples.

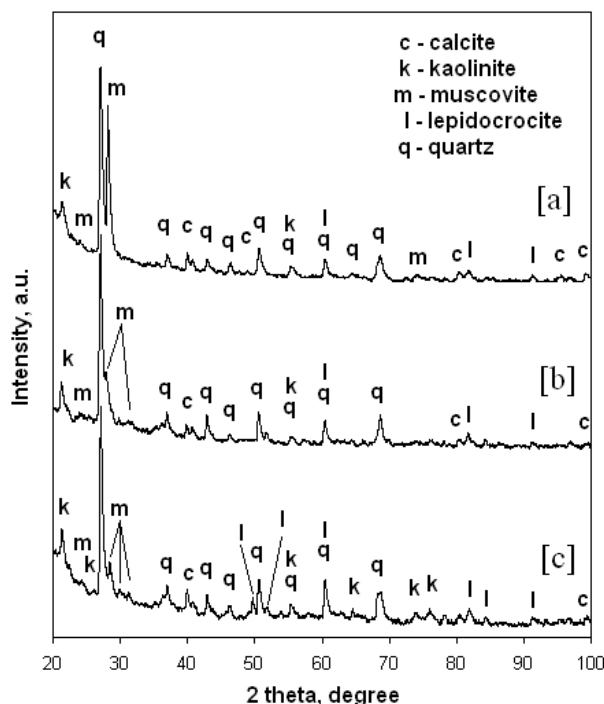


Figure 1. The XRD patterns for SD samples: a) SD1, b) SD2, and c) ASD.

The XRD patterns in figure 1 are similar, only some differences in the peaks relative intensities are observed. It results that all investigated samples (SD1, SD2, and ASD) have the same mineral composition. Quartz is the dominant mineral of SD1 followed by the clay minerals (e.g. muscovite and kaolinite), and also there were found low amount of calcite and lepidocrocite. The average amount of each mineral for ASD sample is given in table 1.

Table 1. ASD minerals characteristics at micro level

Mineral	Amount, Wt. %	Particle size range, μm	Color in cross polarized light
Calcite	10	30 - 150	yellow brown
Kaolinite	10	< 20	light blue
Muscovite	15	< 20	light pink
Lepidocrocite	5	30 - 50	red brown
Quartz	60	50 - 200	green gray

This composition is in good agreement with similar observed in Cluj – Napoca (Hosu Prack et al., 2010; Muntean et al., 2012) and with other big cities in the world (Ferguson & Ryan 1984; Joshi et al., 2009).

Usually, there are two major street dust sources, the natural one from the street adjacent areas degradation, and the anthropogenic one resulted from the built environment decaying (Ferguson & Ryan 1984; Harris 1999). Both sources contribute to the street dust generation in different ratio depending mainly on the human activities developed in the interest area. In our case, Railway Station Square is a high traffic point with large number of cars, buses, and the trains. Such activities erodes adjacent environment such as sidewalks, and green spaces generating significant amounts of ground particles (e.g. quartz, clay, calcite).

At the beginning of the sampling period we observe some infrastructure works at some underground pipes. The old pipes were replaced with new ones and covered by a thick layer of clay mixture for a better isolation and then filled up with ground and asphalted. Clay particles resulted from these activities belongs to the anthropogenic source. This supplementary amount is summed with the clay originating from the natural sources. Fact is proved by the very intense muscovite diffraction peak observed in Figure 1a.

Quartz and calcite are natural compounds often found in the ground (Hosu Prack et al., 2010; Muntean et al., 2012). Lepidocrocite is an iron hydroxide which belongs to the anthropogenic sources (Muntean et al., 2012; Zajzon et al., 2013). Small amount found in ASD is caused by the intensive traffic in the area. Lepidocrocite source in ASD is the rust of cars body and metallic structures

(e.g. rails, metallic gates and walls) (Muntean et al., 2012).

Particle size is the most important parameter for granulated materials, even for the street dust. The result of particle distribution is presented in figure 2. There appears a half of Gaussian distribution having a maximum for the bigger particles. It results that 60.84% wt. have a diameter bigger than 200 μm .

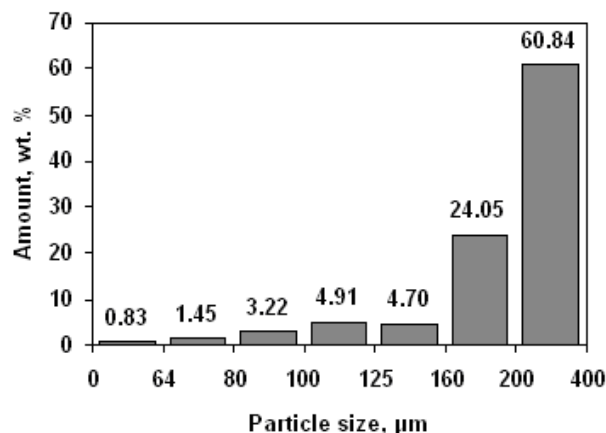


Figure 2. The ASD particle distribution according their size.

Such particles are instantly sedimented in both aqueous and air dispersion, having less harmful potential for health. The other particles situated below 200 μm present relative harmful potential depending on the weather condition (e.g. wind intensity, air humidity). Their microstructure is presented in figure 3.

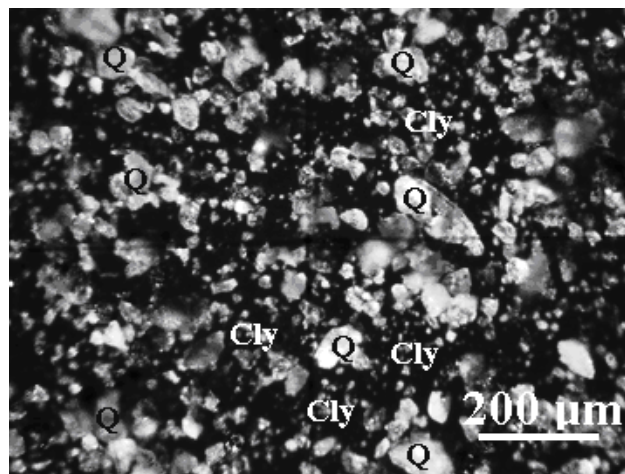


Figure 3. Dark field optical microstructure of ASD particles below 200 μm diameter, quartz bigger particles (Q) and clay finest particles (Cly).

It features a wide spread of particles with different morphology spheroid with, and without sharp edges like quartz, fine lamellar particles like clay one.

The micro –dispersion in figure 3 reveals a lot

of fine particles embedding the larger one having a diameter in the range of 50 – 150 μm . The most dangerous particles are the finest one. These are situated in the category of air sedimenting particles (ASP) (Muntean et al., 2012). The quantitative distribution in figure 2 shows an amount of 0.83 % wt. only. This is in a good agreement with the aspects revealed by microscopy in figure 3.

The maximum limit accepted for air sedimenting particles (SP) in Romania is 17 $\text{g}/\text{m}^2/\text{month}$, according to STAS 10195-75, adapted to the EU environmental regulations (EC Directive 2008/50; Schiopu 2010).

The ASP amount calculation is useful. It could be approached considering the characteristics previously observed for ASD. It is a monthly representative sample, and the finest particle weight percentage is known. Only variable is the total mass of the street dust collected on a square meter.

We have considered several quantities of street dust on square meter in the range of 200 – 3500 g. The histogram is presented in figure 4. It results that the critical amount is about of 2 kilograms per square meter for each street dust similar with our ASD. The maximum level accepted by standards is achieved at this critical amount; at higher amounts the limit is exceeded.

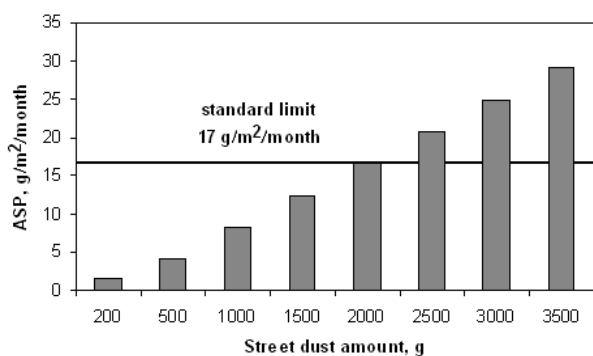


Figure 4. ASP amount dependence on ASD quantity.

However, the collected ASD quantity does not exceed 1.5 kilograms on square meter. It means that the maximum possible emission of ASP is around 10 $\text{g}/\text{m}^2/\text{month}$, significantly below the standard limit. This value is in good agreement with other published values (Mrkajic et al., 2010; Sipos & May 2013).

It is interesting to establish a connection between particle distribution, their shape and mineral composition. The optical mineralogical microscopy is able to differentiate different crystal particles due to their different behavior in the transmitted cross polarized light (Kokhanovsky & Jones 2002; Câmpean et al., 2012).

ASD sample was investigated by both transmitted and cross polarized light microscopy, results are presented in figure 5a and 5b. The dust is evidenced with high contrast in transmitted light, figure 5a; there appear spheroid particles surrounded by fine particles with a lamellar shape. The evidenced morphology and particle sizes are in strong agreement with the dark field microscopy in figure 3.

Crystal particles appear in there bright colored on a darken background. The color and particle size range is given in table 1. Most of the bigger particles observed belongs to the quartz, meanwhile the finest particles belongs to the clay categories.

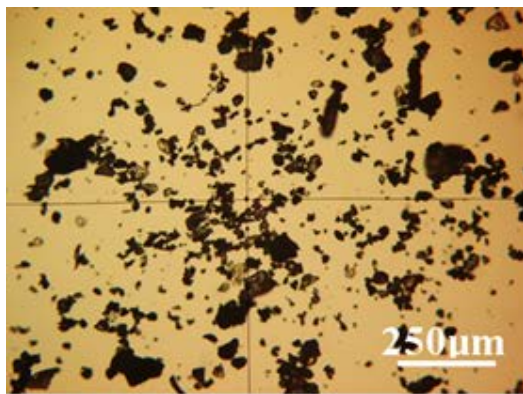
ASP particles could be observed in cross polarized light only at high magnification, (Fig. 5c). Quartz particles are revealed, the bigger ones features sharp edges and the smaller are rounded. There are also revealed two red brown lepidocrocite particles and some calcite particles having an average diameter of 30 μm , some of them could be slightly bigger. The particle size range for the minerals observed is presented in table 2.

Table 2. Small micro-particles characteristics

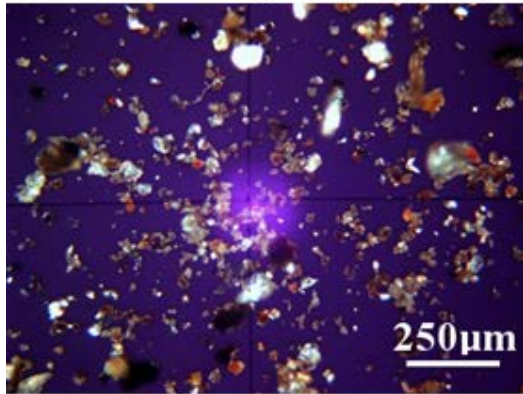
Mineral	Particle diameter range, μm	
	ASP	PTL
Calcite	30 - 50	20 - 25
Kaolinite	<25	5 - 20
Muscovite	<25	5 - 20
Lepidocrocite	30 - 50	-
Quartz	30 - 50	20 - 25

Figure 5c is typical for an APS sample; the features are in strong concordance with literature (Muntean et al., 2012). Such APS usually have significant amount of PM 10 and PM 2.5, and possibly submicron particles. It is difficult to observe such fine particles under optical microscopy, even in cross polarized light. There needs special sample preparation. We use the vertical adsorption from ASD dispersion in deionized water.

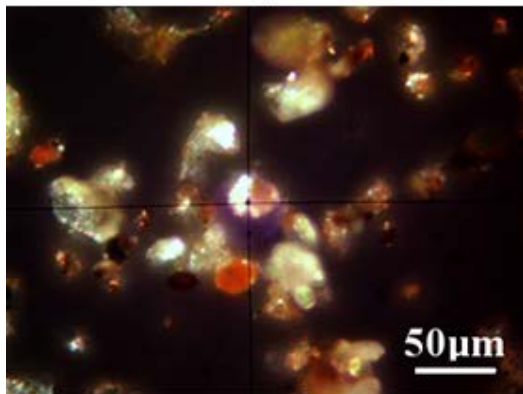
The resulted thin film (particle thin layer – PTL) was further investigated. It is more suitable for the finest particle observation in transmitted light the resulted microstructure is presented in figure 5d. There are evidenced mainly lamellar particles (e.g. clay) having a planar average diameter of 20 μm . The particle thickness do not exceed more than few μm due to their particularly lamellar geometry. It also appears fine dots having around 1 μm and below. This proves to be nano particles arrangements and needs further special investigation techniques like AFM.



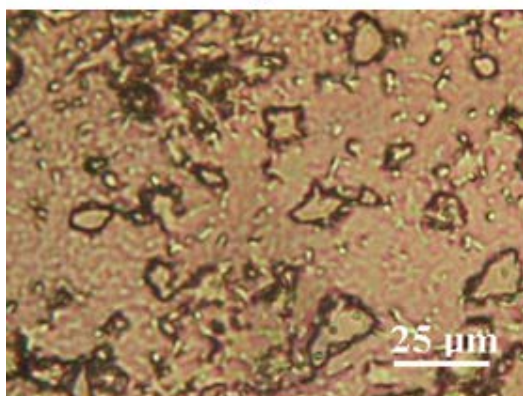
a



b



c



d

Figure 5. Optical microstructure of: a) ASD in transmitted light, b) ASD in cross polarised light, c) ASP in cross polarized light, and d) particle thin layer (PTL).

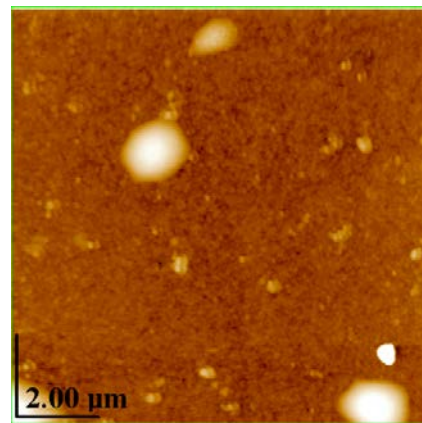


Figure 6. AFM topographical 2D image of PTL sample adsorbed on glass, large scanning area 10 μm x 10 μm.

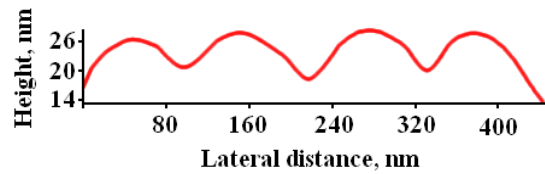
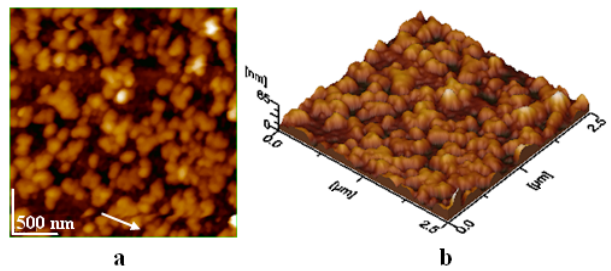


Figure 7. AFM images of the PTL formed on the glass surface: a) topography image, b) 3D view of topography image, c) cross section on the white arrow in image (a). Scanned area 2.5 μm x 2.5 μm.

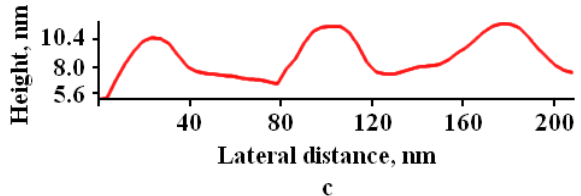
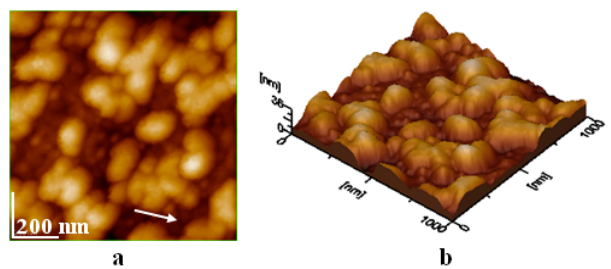


Figure 8. AFM images of the smallest particles in the PTL formed on the glass surface: a) topography image, b) 3D view of topography image, c) cross section on the white arrow in image (a). Scanned area 1 μm x 1 μm.

AFM allows the high resolution imaging of nanoparticles due to the tip – sample interaction (Bowen & Hilal 2009). Adsorbed nanoparticles on

solid substrate (e.g. glass) assure a proper condition for the AFM imaging (Tomoaia et al., 2011; Mocanu et al., 2012). The surface height is probed by this special investigation technique resulting topographical images, allowing an advanced particle characterization at the nano – level.

The topographical AFM image taken on the lower areas of the PTL sample is presented in figure 6. The scanned area (10 μm x 10 μm) was selected between small micro – particles featured in figure 5 to reveal the sample ultra-structure. We found that small dots in observed in figure 5 are in fact small zones with multi – layer adsorption having an circular shape with diameter in the range of 1 – 1.5 μm . These areas are surrounded by monolayer of street dust nano – particles.

Spherical like particles (e.g. quartz) are evidenced forming a random oriented layer, (Fig. 7a). The nano- particle distribution is better observed in the 3D representation of topographic image, (Fig. 7b). The cross section, (Fig. 7c), reveals the particle outer most shape and allows us to calculate the average diameter, (Table 3).

A closer look to the street dust nano-particle layer makes us to believe that is not the end of the smaller particle quest. The small area investigation (e.g. 1 μm x 1 μm) reveal that the above mentioned particle layer is surrounded by small nanoparticles. These are revealed in the AFM topographic image presented in figure 8a and better viewed in the 3D image, (Fig. 8b). The cross section performed along these finest particles, (Fig. 8c), allows us to calculate their average diameter. Resulted value is presented in table 3. This is a tangible prove of nano – scale particulate matters found in the ASD sample.

Further, it is interesting which of the identified mineral belongs those nano – scaled particles. This purpose was fulfilled by an XRD investigation of PTL sample. We carried out two patterns considering first an average range of diffraction angles, (Fig. 9a), and the second pattern was registered at low diffraction angles catching the most representative peaks of the resulted minerals.

Table 3. PTL nano-particles diameter

Mineral	Particle diameter, nm		
	AFM	XRD	rounded value
Kaolinite	40 \pm 5	46.92	45
Muscovite	40 \pm 5	40.90	45
Quartz	90 \pm 5	94.87	95

It is not a surprise that we found relevant diffraction peaks for all minerals observed in ASD sample but their intensities are significant changed due to the adsorption tendency of each mineral type.

Now, the dominant mineral is muscovite, followed by kaolinite and at least relevant is quartz. The other minerals such calcite and lepidocrocite are situated at trace level.

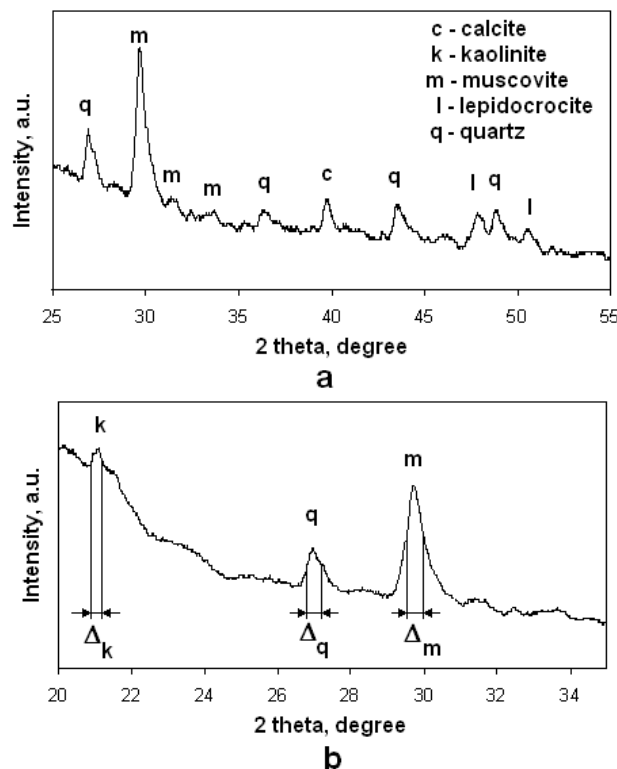


Figure 9. The XRD patterns for PTL: a) average angle range, and b) low angle range detail, Δ is the FWHM of the diffraction peaks.

A diffraction peak broadening involves due to the fine particles found in PTL sample, it is normally due to their interaction with X-ray incident beams. The diffraction peaks broadening due to the dust fine particles were also reported (Pitawala et al., 2013).

All these mineral particles do not feature mechanical stress at the crystal lattice level, than the Scherrer formula is suitable for the calculation of the particle size (Petean et al., 2010; De Poel et al., 2014).

The particle diameter resulted for each mineral is presented in table 3. The values are in a strong concordance with the AFM investigation. Now, we can identify that the nodules of PTL adsorbed monolayer are ultra – fine quartz particles and the surrounding particles are muscovite and kaolinite. Their ability to form air dispersion is expected to be high. Such fine aerosols increase the importance of PM1 as major polluting risk. The interest in PM1 increases mainly to the improvement of scientific investigation tools (Giorio et al., 2013; Shi et al., 2014). The behavior observed for street dust, which can induce nano – particles into the

atmosphere even in the late autumn season, is the starting point for an enlarged new study. This new study will be developed for six months starting with October 2015. The street dust samples will be correlated with PM collected from air.

4. CONCLUSIONS

The street dust found in Railway Station Square Cluj-Napoca during 2010 autumn contains particles derived from natural and anthropogenic sources. The minerals found are quartz, muscovite, calcite, kaolinite and lepidocrocite. This is a normal composition for an urban street dusts, minerals like quartz, muscovite, calcite and kaolinite deriving from natural sources and lepidocrocite from anthropogenic sources. Minerals amount in the individual ASD sample vary according to the human activities developed in the area at the sampling period.

The particle distribution analysis reveals that 0.83 % of total amount of the street dust is able to form air sedimentary particle dispersion (ASP). Ultra fine particles were found among ASP and were evidenced by adsorption from aqueous dispersion on solid substrate (e.g. glass). The resulted particle thin film is formed by quartz particles having 95 nm diameter surrounded by clay particles having an average diameter around of 45 nm.

This behavior of street dust proves to be typical for autumn season. It is the starting point for an enlarged new study developed for six months beginning with October 2015.

Acknowledgements

One of the authors, Alexandra Gertrud Hosu Prack, acknowledges the financial support from UEFISCDI through the grant no. 171.

REFERENCES

Bowen, W.R. & Hilal, N., 2009. *Atomic Force Microscopy in Process Engineering*, Elsevier Linacre House, Jordan Hill, Oxford, p. 283.

Buzea, C., Blandino, I.I.C. & Robbie, C., 2007. Nanomaterials and nanoparticles: A source of toxicity, *Biointerphases*, 2, 4, 17 -172.

Carvalho, T.C., Peters, J.I. & Williams, R.O., 2011. Influence of particle size on regional lung deposition – What evidence is there?. *International Journal of Pharmaceutics*, 406, 1–10.

Câmpean, R. F., Petean, I., Băraian, M., Hosu Prack, A.G., Ristoiu, D. & Arghir, G., 2012. *Mineral Particulate Matter from the St. Ana Lake sand Related to the Water Suspensions*, *Carpathian Journal of Earth and Environmental Sciences*, 7, 2, 57 – 66.

De Poel, W., Pinteau, S., Drnec, J., Carla, F., Felici, R., Mulder, P., Elemans, J., Van Enckevort, W., Rowan, A.E., & Vlieg, E., 2014. *Muscovite mica: Flatter than a pancake*. *Surface Science*, 619, 19–24.

European Council, 2008. *Directive 2008/50 of UE Parliament and European Council concerning atmosphere quality and a more clean atmosphere in Europe, 2008*. Official Journal of European Union, RO: L152, 1 – 44.

Ferguson, J.E. & Ryan, D.E., 1984. *The elemental composition of street dust from large and small urban areas related to city type, source and particle size*. *The Science of the Total Environment*, 34, 101-116.

Gidhagen, L., Johansson, H. & Omstedt, G., 2009. *SIMAIR – Evaluation tool for meeting the EU directive on air pollution limits*. *Atmospheric Environment*, 43, 1029–1036.

Giugliano, M., Lonati, G., Butelli, P., Romele, L., Tardivo, R. & Grosso, M., 2005. *Fine particulate (PM_{2.5}–PM₁) at urban sites with different traffic exposure*, *Atmospheric Environment*, 39, 2421–2431.

Giorio, C., Tapparo, A., Scapellato, L.A., Carrieri, M., Apostoli, L., & Bartolucci, G.B., 2013. *Field comparison of a personal cascade impact or sampler, an optical particle counter and CEN-EU standard methods for PM₁₀, PM_{2.5} and PM₁ measurement in urban environment*. *Journal of Aerosol Science*, 65, 111–120.

Harris, D.J., 1999. *A quantitative approach to the assessment of the environmental impact of building materials*. *Building and Environment*, 23, 640-647.

Hartog, J.J., Hoek, G., Peters, A., Timonen, K. L., Ibaldo-Mulli, A., Brunekreef, B., Heinrich, J., Tiittanen, P., Wijnen, J. H., Kreyling, W., Kulmala, M. & Pekkanen, J., 2003. *Effects of Fine and Ultrafine Particles on Cardiorespiratory Symptoms in Elderly Subjects with Coronary Heart Disease*. *American Journal of Epidemiology*, 157, 7, 613-623.

Hosu-Prack, A.G., Petean, I., Arghir, G., Bobos, L.D. & Tomoaia-Cotisel, M., 2010. *Particulate matter found in urban street dust*. *Studia UBB. Chemia*, 55, 3, 93 – 104.

Jancsek-Turoczi, B., Hoffer, A., Nyiro-Kosa, I., Gelencser, A., 2013. *Sampling and characterization of resuspended and respirable road dust*. *Journal of Aerosol Science*, 65, 69–76.

Joshi, U.M., Vijayaraghavan, K. & Balasubramanian, R., 2009. *Elemental composition of urban street dusts and their dissolution characteristics in various aqueous media*. *Chemosphere*, 77, 526–533.

Kokhanovsky, A.A. & Jones, A.R., 2002. *The cross-polarization of light by large non-spherical particles*, *Journal Of Physics D: Applied Physics*, 35, 1903–1906.

- Linkov, I., Bates, M.E., Trump, B.D., Seager, T.P., Chappell, M.A. & Keisler, J.M., 2013.** *For nanotechnology decisions, use decision analysis*, Nano Today, 8, 5 -10.
- Mrkajic, V., Stamenkovic, M., Males, M., Vukelic, D. & Hodolic, J., 2010.** *Proposal for reducing problems of the air pollution and noise in the urban environment*. Carpathian Journal of Earth and Environmental Sciences, 5, 1, 49 – 56.
- Mocanu, A., Pasca, R.D., Tomoaia, Gh., Avranas, A., Horovitz, O. & Tomoaia – Cotisel, M., 2012.** *Selective effect of procaine, tetracaine, and dibucaine on gold nanoparticles*, J. Nanosci. Nanotechnol., 12, 1 - 5.
- Muntean, D.F., Ristoiu, D., Arghir, G., Campean, R.F. & Petean, I., 2012.** *Iron hydroxides occurrence in winter air particulate matters suspensions in Cluj-Napoca, Romania*. Carpathian Journal of Earth and Environmental Sciences, 7, 175-182.
- Pauluhn, J., 2009.** *Retrospective analysis of 4-week inhalation studies in rats with focus on fate and pulmonary toxicity of two nanosized aluminum oxyhydroxides (boehmite) and pigment-grade iron oxide (magnetite): The key metric of dose is particle mass and not particle surface area*, Toxicology, 259, 140–148.
- Petean, I., Arghir, G., Tomoaia-Cotisel, M., Horovitz, O. & Pop, D.A., 2010.** *Nanostructure formation in mechanically alloyed Fe₅Co₉₅ revealed by X - ray diffraction and atomic force microscopy*, Journal of Optoelectronics and Advanced Materials, 12, 10, 2119 – 2125.
- Pitawala, A., Herath, D. & Piyatunga, N., 2013.** *Chemical Characterization of Household Dust in Two Major Cities: Colombo, The Capital and Kandy, The Hill Capital, Sri Lanka*, Carpathian Journal of Earth and Environmental Sciences, 8, 2, 89 – 95.
- Polichetti, G., Cocco, S., Spinali, A., Trimarco, V. & Nunziata, N., 2009.** *Effects of particulate matter (PM₁₀, PM_{2.5} and PM₁) on the cardiovascular system*, Toxicology, 261, 1–8.
- Schiopu, E., C., 2010.** *Monitoring depositing dust imision in the Rovinari area*, Analele Universitatii Constantin Brancusi din Targu Jiu, Seria Inginerie, 3, 516-522.
- Shi, Y., Chen, J., Hu, D., Wang, L., Yang, X., & Wang, X., 2014.** *Airborne submicron particulate (PM₁) pollution in Shanghai, China: Chemical variability, formation/dissociation of associated semi-volatile components and the impacts on visibility*. Science of the Total Environment, 473–474, 199–206.
- Sipos, P. & May, Z., 2013.** *Vertical distribution of metal deposition rates next to a major urban road in Budapest, Hungary*, Carpathian Journal of Earth and Environmental Sciences, 8, 2, 5 – 12.
- Smith, B.R., Zavaleta, C., Rosenberg, J., Tong, R., Ramunas, J., Liu, Z., Dai, H. & Gambhir, S.S., 2013.** *High-resolution, serial intravital microscopic imaging of nanoparticle delivery and targeting in a small animal tumor model*, Nano Today, 8, 126 – 137.
- Tomoaia, Gh., Frangopol, P.T., Horovitz, O., Bobos, L.D., Mocanu, A. & Tomoaia – Cotisel, M., 2011.** *The effect of arginine on gold nanoparticles in colloidal solutions and in thin films*, J. Nanosci. Nanotechnol., 11, 9, 7762 - 7770.
- Vardoulakis, S. & Kassomenos, P., 2008.** *Sources and factors affecting PM₁₀ levels in two European cities: Implications for local air quality management*. Atmospheric Environment, 42, 3949–3963.
- Vecchi, R., Marcazzan, G., Valli, G., Ceriani, M. & Antoniazzi, C., 2004.** *The role of atmospheric dispersion in the seasonal variation of PM₁ and PM_{2.5} concentration and composition in the urban area of Milan (Italy)*, Atmospheric Environment, 38, 4437–4446.
- Williams, M., 2004.** *Air pollution and policy – 1952 – 2002*. Science of the Total Environment, 334– 335, 15–20.
- Zajzon, N., Marton, E., Sipos, P., Kristaly, F., Nemeth, T., Kis-Kovács, V. & Weiszburg, T.G., 2013.** *Integrated Mineralogical And Magnetic Study of Magnetic Airborne Particles from Potential Pollution Sources in Industrial-Urban Environment*, Carpathian Journal of Earth and Environmental Sciences, 8, 1, 179 – 186.
- Yah, C.S., Simate, S.G. & Iyuke, S.E., 2012.** *Nanoparticles toxicity and their routes of exposures*, Pakistan Journal of Pharmaceutical Sciences, 25, 2, 477-491.

Received: 27. 01. 2014

Revised at: 18. 04. 2016

Accepted for publication at: 16. 06. 2016

Published online at: 22. 06. 2016